STUDY ON THE TYPICAL INFLUENCING FACTORS OF GASOLINE VAPOR EXPLOSION IN A CONFINED SPACE

Run Li[1], Yang-fan Cheng[1,2,*], Rong-kang Zhu[2], Zi-han Chen[2], Jian-wei Xu[2]

[1] School of Safety Science and Engineering, Anhui University of Science and Technology, Huainan 232001, Anhui, PR China

[2] School of Chemical and Blasting Engineering, Anhui University of Science and Technology, Huainan, 232001, Anhui, PR China

[*]Corresponding authors; Email: cyf518@mail.ustc.edu.cn

To explore the influencing factors of explosion accidents caused by gasoline leakage in a confined space, the effects of ignition delay time, ignition energy, initial pressure, initial temperature and mass concentration on gasoline vapor explosion pressure and flame propagation velocity were investigated using a 20 L spherical explosion vessel. The dynamic explosion temperature distribution of gasoline vapor was mapped by the colorimetric thermometry, and the results demonstrated that the optimal ignition delay time, ignition energy and mass concentration of gasoline vapor in the confined space were 100 ms, 100 J and 160 g/m^3, respectively. When the initial pressure was 0.11 MPa, the deflagration pressure of gasoline vapor explosion reached the maximum of 1.08 MPa. The influence of the increasing initial temperature on the maximum explosion pressure rise rate of gasoline was greater than that on the explosion pressure and combustion duration. When the mass concentration of gasoline vapor was 160 g/m^3, the flame propagation velocity and average temperature both obtained their maximum values of 1.23 m/s and 2271 K, respectively. The research results were conductive to reveal the mechanism of explosion accidents caused by gasoline leakage in a confined space, and may provide theoretical guidance for safe storage and transportation of gasoline.

Keywords: *Gasoline; confined space; vapor explosion; explosion accident; colorimetric thermometry*

1. Introduction

Gasoline is one of the basic fuels for national industrial construction and widely used in transportation and energy exploitation. However, gasoline belongs to flammable liquid fuels, and there are many possibilities of accidental explosions in the processes of its processing, storage and transportation. When gasoline explodes, a large area of high temperature and high pressure will be formed along with large amounts of oxygen being consumed, which poses a major threat to the safety of personnel and properties. Therefore, the prevention and control of gasoline explosion accidents in the confined space are still urgent problems that need to be solved [1, 2]. The explosion characteristic parameters (lower explosion limit, explosion pressure, explosion pressure rise rate, etc.) of combustible materials are important indicators to characterize their deflagration hazards [3, 4]. The main factors affecting the explosion characteristics of low boiling point flammable liquids are ignition delay time, ignition energy, initial pressure, initial temperature and mass concentration. Studying the

explosion characteristic parameters of low boiling point flammable liquids with varying influential factors would provide theoretical basis for guaranteeing their safe storage and transportation as well as formulating explosion protection measures.

Heilmann et al. [5] deeply studied the influence of ignition delay time on the explosion characteristics of acetone, and found that the explosion pressure of acetone vapor would be greatly improved with the optimal ignition time. Through studying the effect of ignition energy on lean burn of gasoline engine, Shen et al. [6] demonstrated that the increase of ignition energy was beneficial to the efficient utilization of gasoline energy in gasoline engine. Liu et al. [7] studied the explosion characteristics of propane-diluent-air mixture under different initial pressures using a 20 L explosion vessel, and found that the explosion limit of the mixture increased with initial pressure. Liu et al. [8] analyzed the effect of initial oil temperature on the mixed combustion flame of microalgae oil-aviation kerosene and discovered that the increase of initial oil temperature would enhance the combustion rate of the mixed material, while the increasing initial pressure had a negative effect on it. Shi et al. [9] found that mass concentration would seriously affect the flame propagation characteristics of methanol, and combustion was the most violent as the optimal mass concentration was achieved. The previous studies provided experimental ideas and research methods for exploring gasoline explosion characteristics, and it is feasible to reveal the disaster-causing mechanism of gasoline leakage explosion by analyzing the factors that affect gasoline deflagration characteristics.

In recent years, there are relatively very few experimental studies on the combustion and explosion characteristics of gasoline vapor, but mainly focus on theoretical analysis or numerical simulation of gasoline vapor explosions [10-12]. In this study, gasoline fuel was used as the research object, and the gasoline vapor explosion process was simulated by a 20 L liquid explosion vessel equipped with pressure sensors and a high-speed camera. The vapor explosion characteristics of gasoline fuel with different ignition delay time, ignition energy, initial pressure, initial temperature and mass concentrations were studied, and the flame temperature distribution of gasoline was reconstructed by the colorimetric thermometry. The research results would be helpful to reveal the disaster-causing mechanism of gasoline vapor in a confined space.

2. Experimental materials and apparatus

2.1 Experimental materials

The gasoline fuel used in the experiment was $92^{\#}$ gasoline (92 vol.% Isooctane, 8 vol.% n-heptane) produced by China National Petroleum Corporation. Air (21 vol.% O_2 + 79 vol.% N_2, 99.9 vol.% purity) and nitrogen (N_2, 99.9 vol.% purity) were supplied by Hefei Henglong Electric Co., Ltd., China.

2.2 Experimental apparatus.

The facilities used in the experiment were a 20 L spherical explosion vessel (Jilin Hongyuan Scientific Instrument Co., Ltd., China), a liquid heating device (Jiangsu Xiaoxin Thermal Energy Technology Co., Ltd., China), and a programmable logic controller (PLC, Foshan Sensitive Control Technology Co., Ltd., China). As shown in Fig. 1, the liquid fuel explosion test system was mainly composed of 20 L spherical explosion vessel, fuel spray nozzle, ignition electrode, oscillograph and synchronous control system. There were two symmetrical observation windows with a diameter of 14 cm in the 20 L spherical explosion vessel, which was convenient for the high-speed camera (Memrecam HX 3, NAC, Japan) to record the flame shape. The fuel spraying system was mainly composed of two dispersion nozzles, two 70 mL fuel storage tanks, two electromagnetic control valves, two 1.5 L gas storage tanks and two high-pressure gas cylinders. The ignition

system was mainly composed of two pure tungsten electrodes with a gap of 1.5 mm and a spark generator. The spark generator used in the experiment discharged through a continuous pulse circuit. The data acquisition system consisted of a PCB pressure sensor (PCB 113B24, USA) and an oscilloscope (Teledyne Lecroy, HDO4034, USA). The explosion overpressure signal was received by the pressure sensor and recorded by the oscilloscope. The synchronous control system had a programming logic controller, which was used to control the fuel spraying time, ignition delay time and ignition energy. Before ignition, the gas storage tanks were filled with 0.8 MPa air, and the fuel spray time was set as 50 ms to ensure that the liquid could be fully blown into the spherical tank [13]. Each sample was measured at least three times to minimize the experimental error.

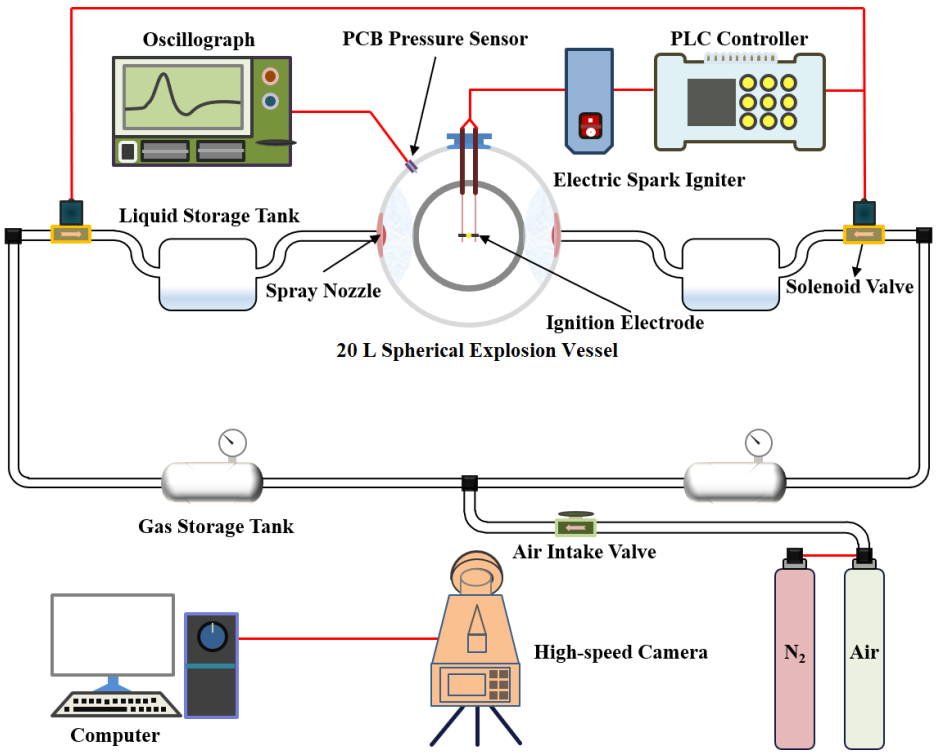

Figure 1. Liquid fuel explosion test system

3. Results and discussion

3.1 Characteristic parameters of gasoline vapor explosion

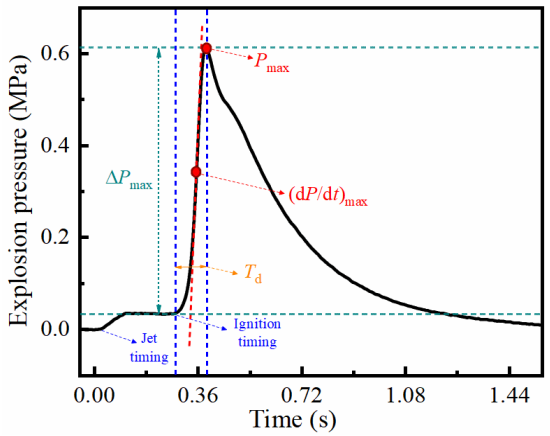

Figure 2. Typical liquid explosion pressure change curve and related definition.

The deflagration characteristics of flammable vapors in confined space can be explained by relevant pressure and time parameters [14]. Fig. 2 is the time history curve of gasoline vapor explosion pressure, which shows that there is a "fluctuation" in the initial stage of pressure rise. The reason for this phenomenon is the action of high-pressure gas in the process of fuel spraying, and the moment of the fluctuation appearing is defined as the spraying starting. Then, there is a platform area in the pressure curve before the explosion pressure begins to rise, and the time period corresponding to the platform is consistent with the ignition delay time of this experiment. Therefore, the time when the pressure begins to rise is determined as the ignition timing. The peak point of the curve is defined as the peak pressure (P_{max}) of the fuel. The time interval between the ignition time and the corresponding time of the peak pressure (P_{max}) is defined as the combustion duration (T_d). The difference between the peak pressure and the pressure at the ignition time is defined as the maximum explosion pressure (ΔP_{max}). After ignition, the maximum slope of the curve during the rise of gasoline explosion pressure is defined as the maximum rate of explosion pressure rise $(dP/dt)_{max}$.

3.1.1 The influence of ignition delay time

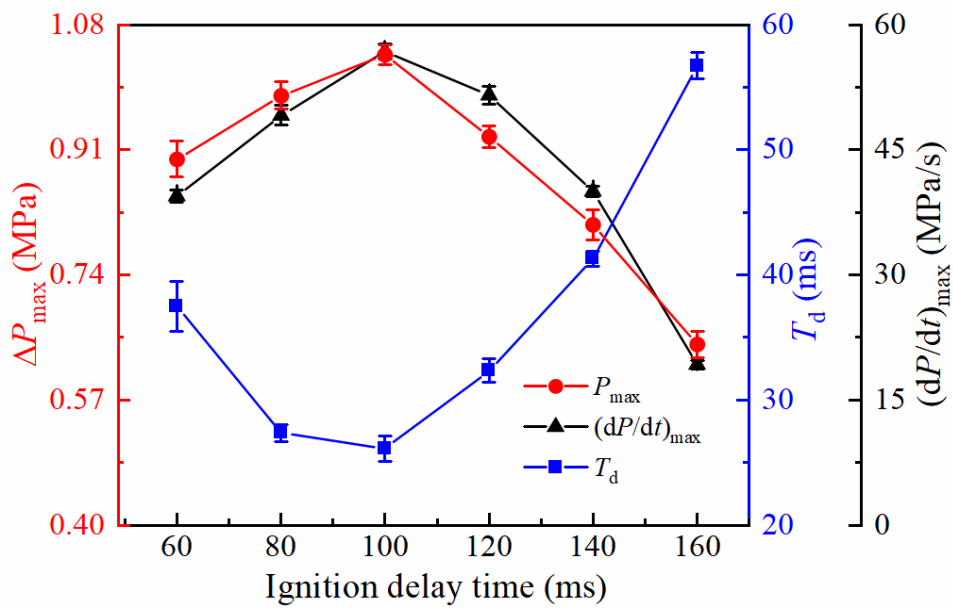

Figure 3. Gasoline explosion parameters under different ignition delay time conditions

Ignition delay time is the time interval between the end of gasoline fuel spraying and the ignition time. In the experiment, the fuel spraying time was set to 50 ms, and the gasoline vapor with a mass concentration of 160 g/m^3 was selected. The effects of different ignition delay times (60, 80, 100, 120, 140 and 160 ms) on the maximum explosion pressure (ΔP_{max}), the maximum pressure rise rate ($(dP/dt)_{max}$) and the combustion duration (T_d) were studied.

Fig. 3 displays the parameters of gasoline explosion under different ignition delay time. It can be seen from the figure that, with the increase of ignition delay time, the maximum explosion pressure and the maximum pressure rise rate of gasoline vapor increased at first and then decreased, and reached the maximum of 1.05 MPa and 57.2 MPa/s, respectively, when the ignition delay time was 100 ms. However, the change trend of combustion duration was opposite, reaching the minimum of 26.5 ms when the ignition delay time was 100 ms. Gasoline droplets were injected into the container through high-pressure air to form a vapor-droplet mixture, which undergone a series of processes such as crushing, dispersion, aggregation and precipitation in the container. The influence of ignition delay time on the explosion was reflected in the uniformity of gasoline cloud dispersion. When the ignition delay time was less than 100 ms, the gasoline

cloud was mixed unevenly. The smaller the ignition delay time was, the greater was the turbulence caused by the high-pressure air in the container. Turbulence will cause gasoline droplets to accumulate in some areas of the container, which will also lead to uneven dispersion of clouds [15]. As the ignition delay time exceeded 100 ms, the dispersion time lasted longer, and the collision between droplets increased, which accelerated the evaporation rate of droplets and reduced turbulence [16]. At the same time, due to the effect of gravity, the sedimentation of droplets was more obvious [17]. Due to the above reasons, the actual concentration of gasoline cloud was lower than the theoretical concentration, resulting in a decrease in the value of explosion characteristic parameters [18].

3.1.2 The influence of ignition energy

Ignition energy refers to the energy that can trigger the chemical reaction of gasoline fuel combustion. Changing the ignition energy will also affect the ΔP_{max} and $(dP/dt)_{max}$ of gasoline vapor explosion [19]. In the experiment, according to the conclusion of section 3.1.1, the ignition delay time was set to 100 ms, and the changes of combustion and explosion characteristic parameters of 160 g/m^3 gasoline vapor under eight different ignition energies (40, 60, 80, 100, 120, 140, 160 and 180 J) were studied.

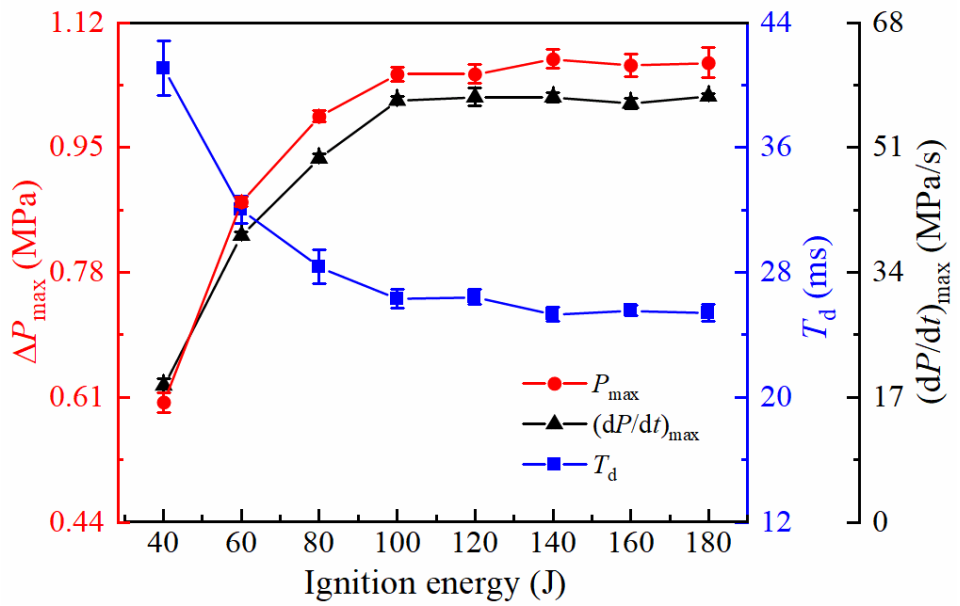

Figure 4. Gasoline explosion parameters under different ignition energy conditions.

Fig. 4 displays that with the increase of ignition energy, the ΔP_{max} and $(dP/dt)_{max}$ values of gasoline fuel increased firstly and then fluctuated gently. The values of ΔP_{max} and $(dP/dt)_{max}$ reached leveling-off point of 1.05 MPa and 57.23 MPa/s, respectively, when the ignition energy was 100 J .However, T_d values showed a trend of decreasing initially and then fluctuating gently, reaching the turning point of 26.5 ms when the ignition energy was 100 J. According to the analysis, the ignition energy was a major factor affecting the initiation process of gasoline vapor. When the ignition energy was less than 100 J, with the increase of ignition energy intensity, the initial heat of spark increased, causing more gasoline droplets to participate in the initial reaction, resulting in larger values of ΔP_{max} and $(dP/dt)_{max}$. When the ignition energy exceeded 100 J, since the mass concentration was fixed, the initial vapor volume that the ignition energy could ignite was close to the peak value. Continuing to increase the ignition energy would not have a significant impact on the combustion and explosion parameters. The fluctuation of the parameters in the later stage was caused by the slight difference in the cooling effect (heat loss) of the steel vessel wall in each experiment [20].

3.1.3 The influence of initial pressure

In the process of transportation and storage, the tank would leave a certain gas space for the gasoline fuel. With the volatilization of gasoline in the interior, the internal pressure of the confined space would increase, which may lead to an accidental explosion. Previous studies had pointed out that the volume ratio of gasoline volatiles could be reduced by adding inert gases to the confined space to suppress accidental gasoline explosion [21]. However, the addition of inert gas also increased the initial pressure of gasoline fuel in the tank, which had a certain impact on the transportation and storage of gasoline. Therefore, in order to study the effect of initial pressure on the combustion and explosion characteristics of gasoline, this study changed the initial pressure (0.10-0.30 MPa) in the 20 L spherical explosion vessel by filling it with different volume fractions of N_2, while keeping the oxygen content in the system unchanged.

Tab. 1 shows the test results of gasoline vapor explosion with the mass concentration of 160 g/m^3 under different initial pressures. The initial pressure of the 20 L spherical explosion vessel increased with the increasing volume fraction of N_2, and meanwhile the proportion of O_2 in mixed gases decreased, which led to the ignition of gasoline fuel more difficult [22]. When the initial pressure was in the range of 0.10-0.14 MPa, the gasoline vapor could undergo a deflagration reaction. When the initial pressure was 0.15 MPa, the gasoline vapor could not be stably ignited. When the initial pressure continued to increase (in the range of 0.16-0.30 MPa), the gasoline vapor could not be ignited. In summary, the limit initial pressure (i.e., the maximum initial pressure when the gasoline vapor can be stably ignited) of gasoline vapor explosion was defined as 0.15 MPa.

Table 1. Continuous test results of limit initial pressure of gasoline explosion.

Serial Number	N_2 Volume Fraction (vol.%)	Initial Pressure (MPa)	Experimental Times				
			I	II	III	IV	V
1	80.0	0.10	√	√	√	√	√
2	81.8	0.11	√	√	√	√	√
3	83.3	0.12	√	√	√	√	√
4	84.6	0.13	√	√	√	√	√
5	85.8	0.14	√	√	√	√	√
6	86.7	0.15	√	×	×	√	×
7	87.5	0.16	×	×	×	×	×
8	90.0	0.20	×	×	×	×	×
9	92.0	0.25	×	×	×	×	×
10	93.3	0.30	×	×	×	×	×

Fig. 5 displays that the values of ΔP_{max} and $(dP/dt)_{max}$ of gasoline explosion increased at first and then decreased with the rise of initial pressure, reaching the maximum of ΔP_{max}=1.08 MPa and $(dP/dt)_{max}$=75.86 MPa/s when the initial pressure was 0.11 MPa. However, T_d decreased firstly and then increased with the rise of initial pressure, and reached the minimum value T_d =22.7 ms when the initial pressure was 0.11 MPa,

where the volume fraction of N_2 was 81.81%. This was because when the initial pressure was less than 0.11 MPa, the increase of the initial pressure would accelerate the chemical reaction ratio, which had a positive effect on the combustion and explosion of gasoline vapor, enhancing the explosion pressure. When the initial pressure was greater than 0.11 MPa, the volume ratio of N_2 continued to increase, and the inhibition effect on the contact between gasoline vapor and O_2 molecules in the tank was gradually prominent and dominant, which had a negative effect on the combustion and explosion of gasoline vapor, and the negative effect exceeded the positive effect caused by the increasing initial pressure, furthermore, the injection speed of gasoline vapor was also reduced to a certain extent, thus prolonging the combustion duration but weaken the explosion pressure [23].

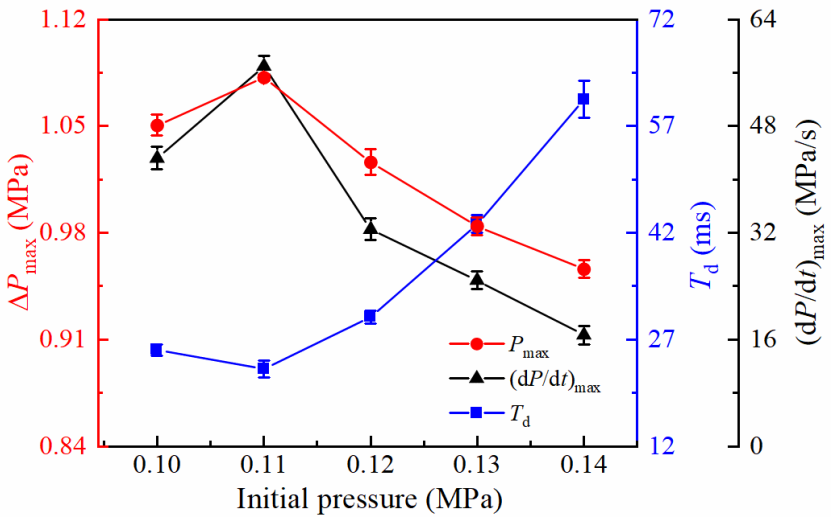

Figure 5. Gasoline explosion parameters under different initial pressure conditions.

3.1.4 Effect of initial temperature

The change of the initial temperature of gasoline fuel would change the state of gasoline fuel. The increase of temperature promoted the evaporation of gasoline, which made the explosion process of gasoline vapor more dangerous and destructive [24, 25]. In the experiments, according to the conclusion of section 3.1.3, the ignition energy was set to 100 J, and the combustion and explosion characteristic parameters of gasoline fuel with mass concentration of 160 g/m^3 under five different initial oil temperatures (283, 298, 313, 328 and 343 K) were studied.

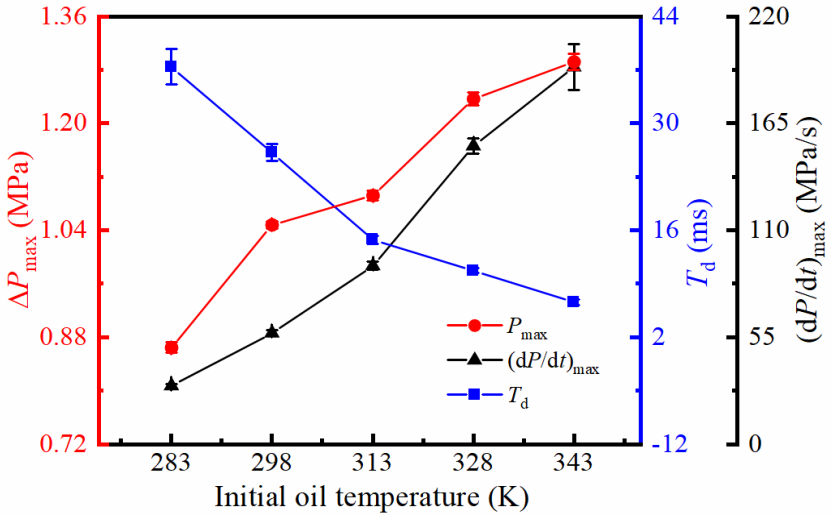

Figure 6. Gasoline explosion parameters under different initial oil temperature conditions.

Fig. 6 displays that the values of ΔP_{max} and $(dP/dt)_{max}$ of gasoline fuel increased continuously with the initial temperatures. Compared with the initial oil temperature of 283 K, the ΔP_{max} and $(dP/dt)_{max}$ values of gasoline fuel increased by 50.2 % and 556 %, respectively, at the initial temperature of 343 K. However, the T_d value of gasoline fuel decreased continuously, and decreased by 82.1% when the initial temperature of gasoline fuel was 343 K compared with 283 K. Therefore, the change of initial oil temperature had a significant effect on $(dP/dt)_{max}$. On one hand, with the increase of initial oil temperature, the volatile light components in gasoline increased, so that the injected fuel contained more gasoline vapor, and the vapor diffused to the whole spherical tank at a faster rate [26]. After the ignition electrode sparked, the existence of gasoline vapor increased the continuous phase in the system, thus accelerating the propagation of flame, increasing the explosion pressure rise rate and reducing the combustion duration. On the other hand, because of the continuous increase in the initial oil temperature, the fuel was transformed from the liquid phase to the gas phase, for the number of gasoline droplets was minimized, less heat would be absorbed inside the 20 L spherical explosion vessel during combustion, so that the heat loss of the system was also reduced [27, 28], thereby promoting the occurrence of gasoline explosion reaction and increasing the maximum explosion pressure. Through experiments, it was found that if gasoline was ignited at a lower temperature, the volatile light components were reduced, which led to the reduction of gasoline explosion risk.

3.1.5 Effect of gasoline vapor mass concentration

Studying the effect of mass concentration on gasoline explosion parameters is helpful to understand and control the gasoline explosion process, improve the fuel utilization efficiency, and reduce the environmental pollution and safety hazards. The effects of six different mass concentrations (60, 110, 160, 210, 260 and 310 g/m^3) on the gasoline vapor explosion parameters were studied by selecting the optimal ignition delay time of 100 ms and the optimal ignition energy of 100 J determined in sections 3.1.1 and 3.1.2.

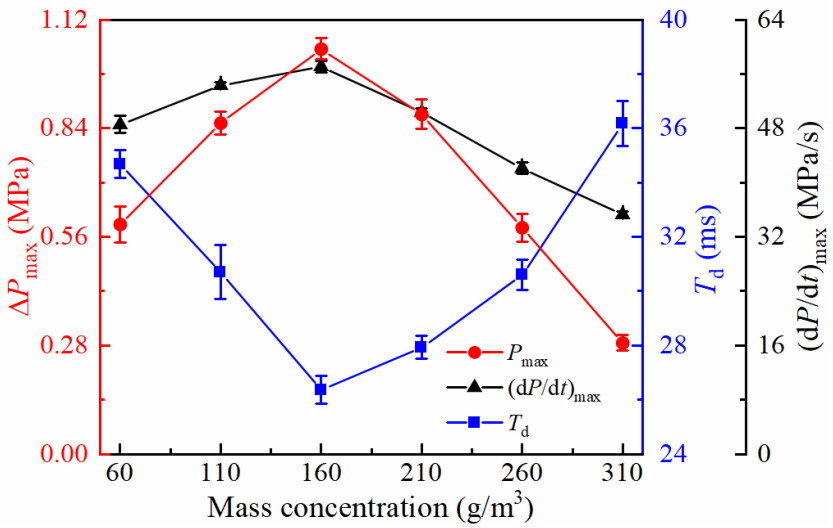

Figure 7. Gasoline explosion parameters under different mass concentration conditions.

Fig. 7 displays the variation curves of combustion and explosion characteristic parameters of gasoline fuel under the different mass concentrations. The ΔP_{max} and $(dP/dt)_{max}$ values of gasoline vapor combustion and explosion increased at first and then decreased with the increase of fuel mass concentration, reaching the maximum of ΔP_{max}=1.05 MPa and $(dP/dt)_{max}$=57.22 MPa/s, respectively, when the mass concentration was 160 g/m^3. The change trend of T_d was opposite, and reached the minimum value (T_d=26.5 ms) as the mass concentration was 160 g/m^3. This was because when the mass concentration was lower than 160 g/m^3, the

amount of oxygen in the tank was sufficient, which could supply gasoline fuel for complete reaction. With the increasing mass concentration of gasoline fuel, the number of gasoline fuel droplets increased, and the effective collision between molecules increased in unit time, which accelerated the reaction rate of gasoline fuel. On the other hand, the gasoline deflagration reaction was a process of heat accumulation. The generated heat would accelerate the subsequent deflagration reaction, thus accelerating the heat release rate, reducing the combustion time but increasing the maximum deflagration pressure and pressure rise rate [29]. When the gasoline fuel exceeded 160 g/m^3, due to the excessive number of gasoline droplets, the aggregation effect was easy to occur between the droplets, which would hinder the reaction processes. The droplets that did not participate in the combustion would absorb the heat released by the prior combustion [30], and the oxygen content in the vessel was insufficient, which decreases the maximum explosion pressure and the maximum pressure rise rate, but increases the combustion duration.

3.2 Flame propagation velocity and temperature characteristics of gasoline vapor flame

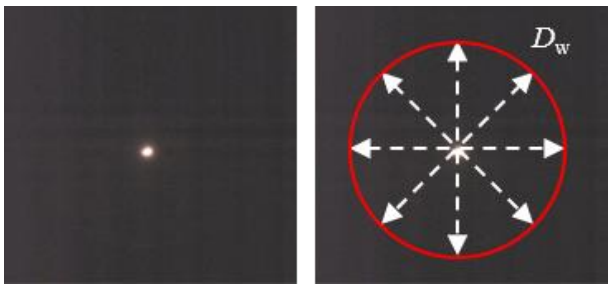

Figure 8. Pixel coefficient calibration process.

Flame propagation velocity is the most intuitive parameter for characterizing the flame propagation process of gasoline fuel. It is of great significance to study the flame propagation velocity of gasoline vapor explosion to explore the risk of gasoline explosion [31]. The flame propagation velocity V of gasoline vapor explosion is the rate of increase of the flame radius r [32]. In previous studies[33-35], the measurement of spherical flame was based on the change of diameter in the horizontal direction to calculate the change of flame propagation velocity. It can be seen from the flame change process obtained by shooting that the flame propagation of gasoline combustion and explosion was not quasi-spherical. Therefore, this paper improves the measurement method, calculates the average value in four directions to obtain the change of equivalent radius, so as to more accurately represent the change of flame propagation velocity. In order to calculate the true radius of flame, it is necessary to calculate the pixel calibration coefficient through calibration experiment (Fig. 8). The following equation is shown as follows:

$$a = \frac{D_w}{d_w} \tag{1}$$

In the formula, a is the pixel coefficient, px/cm ; D_w is the measured pixel length of the observation window diameter, px ; d_w is the actual length of the observation window, cm. The value of the pixel coefficient a is calculated to be 18.57 px/cm.

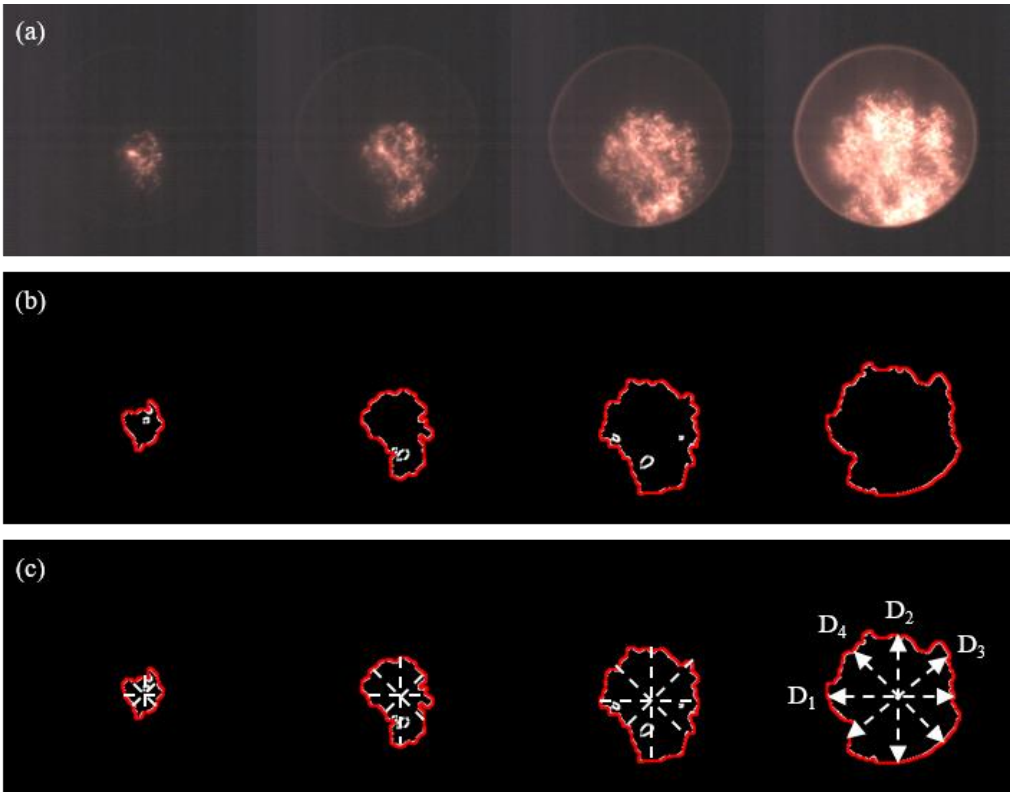

Figure 9. Flame edge detection and measurement process diagram.

In the experiments, a high-speed camera was used to capture the flame propagation diagram at a frame rate of 4000 fps, as shown in Fig. 9(a), and the flame edge detection technology based on a Python code was used to detect the contour of gasoline vapor deflagration flame, as shown in Fig. 9(b). Finally, the diameters of D_1, D_2, D_3 and D_4 of the deflagration flames in four directions (horizontal, vertical, +45°, −45°) were measured and the equivalent diameter D was calculated to obtain the flame radius r, as shown in Fig. 9(c).

$$R = D \times \frac{1}{2} = \frac{D_1 + D_2 + D_3 + D_4}{4} \times \frac{1}{2} \tag{2}$$

$$r = d \times \frac{1}{2} = \frac{R}{\mathrm{a}} \tag{3}$$

In the equations (2) and (3), R is the pixel length of the measured flame equivalent radius, px ; D is the measured flame equivalent diameter pixel length, px ; D_1, D_2, D_3 and D_4 are the measured flame diameter pixel length in four directions, px ; r is the actual flame radius, cm ; d is the actual flame diameter, cm.

$$V = \frac{\Delta r}{\Delta \mathrm{t}} \tag{4}$$

$$V_{ave} = \frac{\sum_{1}^{i} V}{i} \tag{5}$$

In the equations (4) and (5), V is the velocity of spherical flame propagation, m/s ; Δr is the difference of flame radius between two adjacent frames, cm ; Δt is the time interval between two adjacent frames, 0.25 ms ; i is the number of points calculated ; V_{ave} is the average flame propagation speed, m/s.

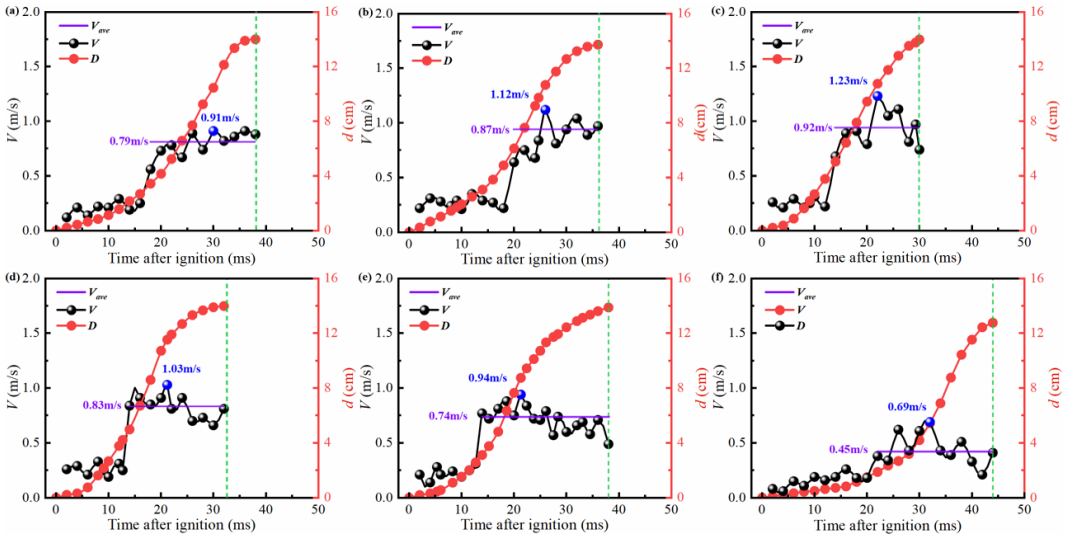

Figure 10. Flame propagation process and flame width at different mass concentrations of gasoline: (a) 60 g/m^3; (b) 110 g/m^3; (c) 160 g/m^3; (d) 210 g/m^3; (e) 260 g/m^3 and (f) 310 g/m^3.

Fig. 10 indicates that the flame propagation distance continues to increase after the gasoline fuel was ignited. As a whole, the flame propagation speed showed a trend of rising firstly and then falling. At the same time, it can be seen from the figure that the flame propagation speed fluctuated up and down in the process of gasoline explosion, which was caused by the periodic thermal radiation in the process of flame propagation. Through experiments, it was found that the flame propagation velocity in the process of gasoline vapor explosion will have a small amplitude of oscillation, which was similar to Wang et al. ' s [36] work. It was also due to the influence of the thermal radiation of the wall and the droplets during the flame propagation process, which affected the flame structure and thus affected the flame propagation velocity, but it did not affect the overall trend of flame propagation speed in this process.

In addition, the time corresponding to the green dotted line in Fig. 10 was the time required for the combustion flame to grow to a diameter of 14 cm (the width of the observation window), which shows that the time for the flame to reach the edge of observation window decreased at first and then increased with the increasing mass concentration of gasoline vapor. At the same time, as shown in Fig. 11, combined with the scatter diagram and trend fitting diagram of the maximum flame propagation velocity (V_{max}) and the average flame propagation velocity (V_{ave}) of gasoline explosion at different mass concentrations, it can be seen that both V_{max} and V_{ave} increased firstly and then decreased with the increase of gasoline mass concentration, and reached the peak values at 160 g/m^3 (V_{max} = 1.23 m/s, V_{ave} = 0.92 m/s). This was because when the mass concentration of gasoline was less than 160 g/m^3, the oxygen content in the tank was sufficient. With the increase of mass concentration, more fuel would be involved in the reaction, and the molecular gap of the droplets became smaller, so that the development of the explosion flame was more continuous, leading to the acceleration of gasoline explosion flame. When the mass concentration of gasoline was larger than 160 g/m^3, the O_2 in the spherical tank was not enough to support the explosion reaction of all gasoline droplets. The unburned gasoline droplets would continue to absorb the heat generated in the system, thereby reducing the speed of gasoline combustion flame propagation [37]. This was different from the work of Wang et al [38], he studied the pure gas explosion, this paper studied the gasoline vapor explosion. However, the generation of the optimal mass concentration was related to the air-fuel ratio. When the mass concentration exceeded the optimal mass concentration, the gasoline vapor that was not in contact with oxygen and completely explodes will absorb the heat generated by the reaction, which will reduce the average temperature and slow down the reaction.

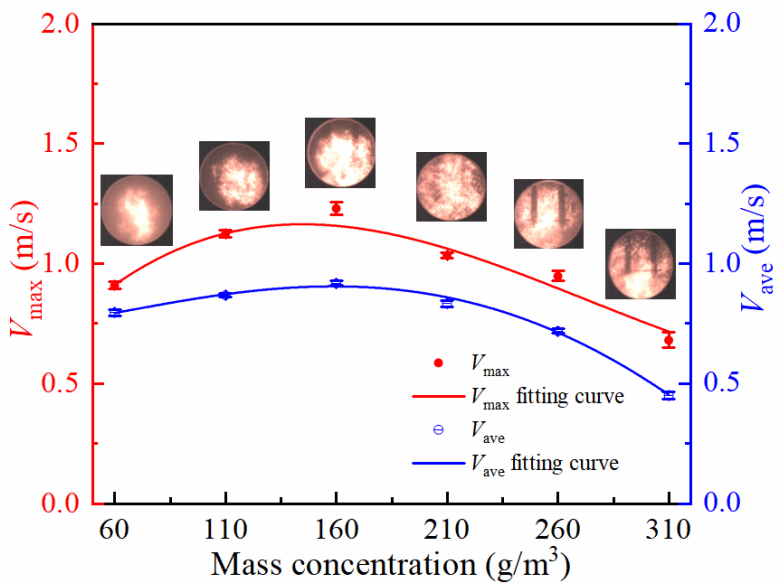

Figure 11. V_{max} and V_{ave} scatter plots and trend fitting plots of gasoline explosion at different mass concentrations.

3.3 Gasoline vapor combustion flame temperature

Deflagration temperature is also an important parameter to reflect explosion hazard of gasoline. In recent years, our group has carried out a lot of research on the temperature measurement of explosive, gas and dust explosion by the colorimetric thermometer based on the black-body radiation law [39]. This method has the advantage of fast response, high measurement accuracy and strong anti-interference ability, which make it superior to the traditional non-contact temperature measurement methods. The contact temperature measurement method requires the thermometer to contact with the liquid, which may lead to inaccurate measurement of temperature, and may affect the flame propagation and pressure during use. Therefore, this study used the colorimetric thermometer to map the temperature field of gasoline vapor explosion flame, and study the temperature distribution evolution of gasoline vapor explosion flame under different mass concentrations.

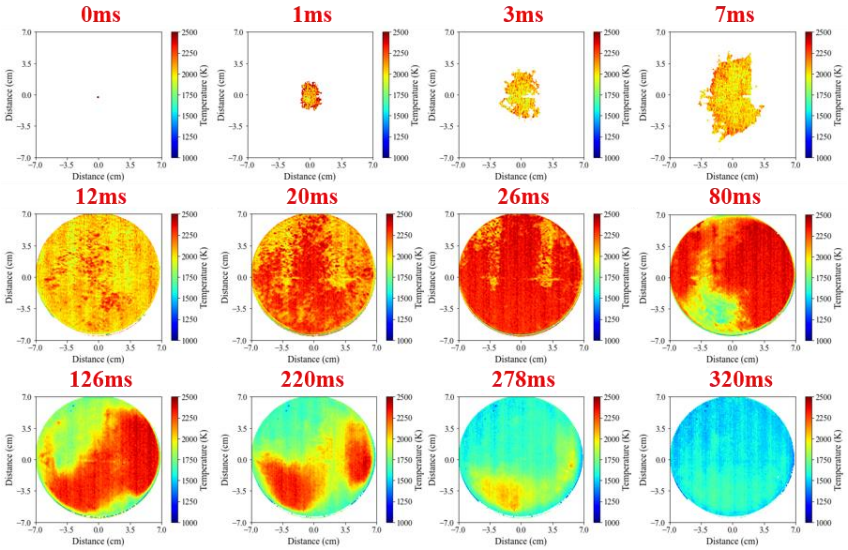

Figure 12. The temperature change diagram of gasoline vapor deflagration flame with mass concentration of 160 g/m^3.

Fig. 12 shows the temperature distribution of gasoline vapor explosion flame with a mass concentration of 160 g/m^3. When t = 0-12 ms, the dispersed gasoline droplet explosion flame in the spherical tank spread outward from the ignition center, and the measured temperature field also spread outward. When t = 12-16 ms, the flame spread from the central region to the whole vapor, and the flame temperature also rose sharply, where the highest average temperature reached 2271 K. After t = 16 ms, the sedimentation effect of gasoline droplets increased the concentration of gasoline vapor in the lower part of the spherical tank, and the violent explosion reaction led to the increase of heat release in this zone, which made the temperature there relatively higher, showing that the area with temperature higher than 2000 K gradually extended to the lower part of the spherical tank. As the combustion reaction continued, the reaction of fuel and oxygen in the system was exhausted, the flame was gradually extinguished, and the combustion temperature was also gradually reduced [40].

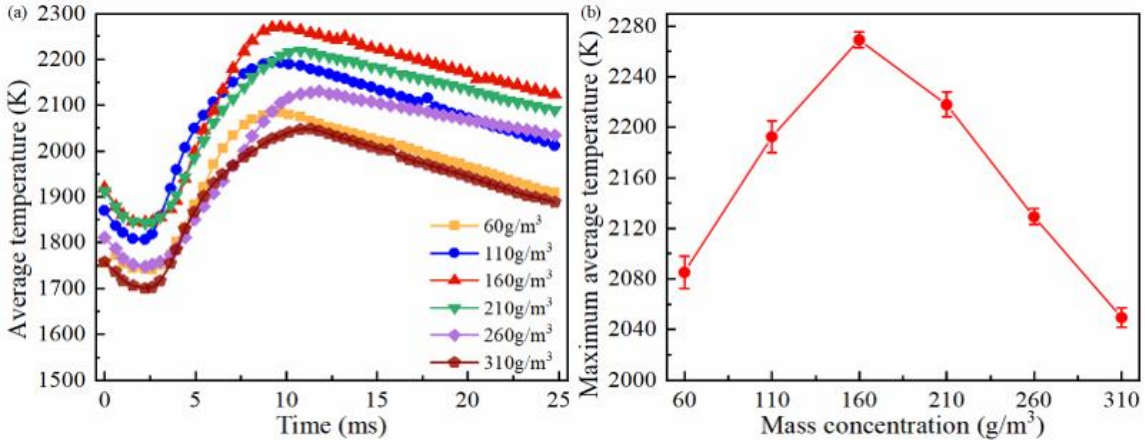

Figure 13. Gasoline vapor deflagration flame temperature under different mass concentrations: (a) Flame temperature change time history curve; (b) Maximum average temperature variation diagram.

By averaging the values of effective temperatures corresponding to each pixel in the flame temperature field distribution diagram, the average temperature of gasoline flame at different times was obtained. Fig. 13 is the time-history curves of flame temperature and the maximum average temperature curve of gasoline vapor explosion flame with different mass concentrations. Fig. 13(a) shows that the gasoline vapor explosion temperature presented a trend of "decline-rise-decline" with time. After the gasoline vapor was ignited, the heat generated in the initial stage of the reaction was decreased, and the unburned gasoline droplets would absorb the heat released by the burned area, so the temperature decreased in a small range [41]; when the flame propagated to the whole spherical vessel, the gasoline vapor gathered and burnt, resulting in a sharp rise in temperature. After the temperature reached its peak value, the temperature began to decrease gradually because that the rate of heat loss was higher than the rate of heat release in the deflagration reaction [42]. Fig. 13(b) shows that with the increase of the mass concentration of gasoline vapor, the maximum average temperatures of the flame increased at first and then decreased, which were 2083, 2193, 2271, 2219, 2130 and 2048 K, respectively, reaching the highest value of 2271 K when the mass concentration was 160 g/m^3, corresponding to the change trend of the flame propagation speed of gasoline vapor.

4. Conclusions

In this study, a 20 L spherical liquid explosion test device was used to study the effects of ignition delay time, ignition energy, initial pressure, initial oil temperature and mass concentration on the combustion and explosion characteristics of gasoline fuel in a confined space. The main conclusions are as follows:

With the increase of ignition delay time, ΔP_{max} and $(dP/dt)_{max}$ of gasoline vapor explosion increased firstly and then decreased, while T_d decreased initially and then increased. The optimal ignition delay time and mass concentration were 100 ms and 160 g/m^3, respectively. With the increase of ignition energy, ΔP_{max} and $(dP/dt)_{max}$ increased at first and then changed smoothly, while T_d decreased initially and then changed smoothly, and the optimal ignition energy was 100 J.

With the increase of initial pressure, the ΔP_{max} and $(dP/dt)_{max}$ of gasoline vapor increased firstly and then decreased, while T_d showed the opposite trend, and the optimal initial pressure was 0.11 MPa. The effect of initial temperature on the $(dP/dt)_{max}$ of gasoline vapor explosion was much higher than that of ΔP_{max} and T_d. As the initial oil temperature increases from 283 K to 343 K, the maximum pressure rise rate of gasoline explosion increased by 556 %.

With the increase of mass concentration, the flame propagation velocity of gasoline vapor explosion increased firstly and then decreased. The optimum mass concentration was 160 g/m^3, and the average flame propagation velocity reached V_{max} = 1.23 m/s. The explosion temperature of gasoline vapor showed a trend of "down-up-down" along with the time. The maximum average temperature increased firstly and then decreased with the mass concentration of gasoline vapor, reaching the maximum average temperature of 2271 K when the mass concentration was 160 g/m^3.

Acknowledgments

Many thanks to Prof. Ritsu Dobashi, Dr. Po-Jul Chang of the University of Tokyo, for their kindness help with the two-color pyrometer technique. This work was supported by National Natural Science Foundation of China (No.12272001), and Natural Science Research Excellent Youth Project of Anhui Educational Committee (No.2023AH020026), and Anhui University of Science and Technology Postgraduate Innovation Fund (2023CX2022), and the authors would like to thank these foundations for the financial supports.

References

[1] G. Li, X. Wang, X. Zhao. Experimental study on explosion characteristics of ethanol-gasoline blended fuels. Journal of Loss Prevention in the Process Industries. 64 (2020), 104083.

[2] R. Küçükosman, H. Değirmenci, A. A. Yontar. Combustion characteristics of gasoline fuel droplets containing boron-based particles. Combustion and Flame. 255 (2023), 112887.

[3] X. Wang, E. Shi, C. Qi. Experimental study on aerosol explosion characteristics and flame propagation behavior of aluminum/ethanol nanofluid fuel. Fuel. 352 (2023), 129022.

[4] S. Guo, F. Wu, H. Wang. Evolution characteristics of ethyl ether spray explosion process in 20L near-spherical vessel. Fuel. 357 (2024), 129736.

[5] V. Heilmann, S. Zakel, D. Gabel. Influence of different ignition delay times on the pressure rise rate in hybrid mixture explosions in the 20-L sphere. Journal of Loss Prevention in the Process Industries. 84 (2023), 105106.

[6] K. Shen, Z. Xu, H. Chen. Combined effects of high energy ignition and tumble enhancement on performance of lean combustion for GDI engine. Experimental Thermal and Fluid Science. 129 (2021), 110464.

[7] J. Liu, C. E. Dumitrescu. Analysis of two-stage natural-gas lean combustion inside a diesel geometry.

Applied Thermal Engineering. 160 (2019), 114116.

[8] Y. Liu, Y. Zhang, D. Zhao. Effects of initial temperature and pressure on explosion characteristics of propane–diluent–air mixtures. Journal of Loss Prevention in the Process Industries. 72 (2021), 104585.

[9] E. Shi, J. Yu, C. Qi. Explosion characteristics and reaction mechanism of nano-aluminum/methanol fuel spray in a square closed vessel. Fuel. 357 (2024), 129928.

[10] J. Kang, Z. Wang, H. Jin. Dynamic risk assessment of hybrid hydrogen-gasoline fueling stations using complex network analysis and time-series data. International Journal of Hydrogen Energy. 48 (2023), 30608-30619.

[11] G. Li, K. Zheng, S. Wang. Comparative study on explosion characteristics of hydrogen and gasoline vapor in a semi-confined pipe based on Large Eddy Simulation. Fuel. 328 (2022), 125334.

[12] A. Galeev, Y. Chistov, S. Ponikarov. Numerical analysis of flammable vapour cloud formation from gasoline pool. Process Safety and Environmental Protection. 137 (2020), 211-222.

[13] H. W. Wan, Y. Q. Wen, Q. Zhang. Explosion behaviors of vapor–liquid propylene oxide/air mixture under high-temperature source ignition. Fuel. 331 (2023), 125815.

[14] J. Cheng, B. Zhang. Analysis of explosion and laminar combustion characteristics of premixed ammonia-air/oxygen mixtures. Fuel. 351 (2023), 128860.

[15] X. Song, H. Su, Xie. L, et al. Experimental investigations of the ignition delay time, initial ignition energy and lower explosion limit of zirconium powder clouds in a 20 L cylindrical vessel. Process Safety and Environmental Protection. 134 (2020), 429-439.

[16] L. Zhan, H. Chen, H. Zhou, et al. Droplet-particle collision dynamics: A molecular dynamics simulation. Powder Technology. 422 (2023): 118456.

[17] V. Heilmann, S. Zakel, D. Gabel, et al. Influence of different ignition delay times on the pressure rise rate in hybrid mixture explosions in the 20-L sphere. Journal of Loss Prevention in the Process Industries. 84 (2023), 105106.

[18] W. Sun, J. Ji, Y. Li. Dispersion and settling characteristics of evaporating droplets in ventilated room. Building and Environment. 42(2) (2007), 1011-1017.

[19] Y. B. Chen, Z. Yang, Z. Lv. Effect of ignition energy on combustion characteristics of flammable working fluids. Fuel. 335 (2023), 127022.

[20] T. Zhang, J. F. Zhang, Z. Lv. et al. Insight into energy release characteristics of TiH2 dust explosion through ignition experiments and molecular dynamic simulations. Process Safety and Environmental Protection. 185 (2024), 853-863.

[21] C. Liu, K. Tang, C. Huang. Effect of initial pressure on the critical characteristics and overpressure of hydrogen-air premixed gas combustion and explosion. International Journal of Hydrogen Energy, 49 (2023), 311-322.

[22] S. Li, Y. F. Cheng, R. Wang, et al. Suppression effects and mechanisms of three typical solid suppressants on titanium hydride dust explosions. Process Safety and Environmental Protection, 177 (2023): 688-698.

[23] R. J. Sornek, R. Dobashi, T. Hirano. Effect of turbulence on vaporization, mixing, and combustion of

liquid-fuel sprays. Combustion and Flame, 120(4) (2000): 479-491.

[24] H. Zhang, Z. Lu, T. Wang. Mist formation during micro-explosion of emulsion droplets. Fuel, 339 (2023): 127350.

[25] S. Wang, D. Wu, H. Guo. Effects of concentration, temperature, ignition energy and relative humidity on the overpressure transients of fuel-air explosion in a medium-scale fuel tank. Fuel, 259 (2020): 116265.

[26] C. Qi, X. Yu, Y. Wang . Investigating the effect of temperature, pressure, and inert gas on the flammability range of ethane/oxygen mixtures. Fuel. 354 (2023), 129296.

[27] G. Zhang, J. Guo, J. Zhang. Experimental study on flame propagation through stratified crude oil vapor in a horizontal duct. Fuel, 294 (2021), 120531.

[28] C. Zhang, C. H. Bai, J. Yao. Liquid component effect on the dispersion and explosion characteristics of solid-liquid mixed fuel. Fuel. 319 (2022), 123806.

[29] H. Wang, F. Wu, X. Pan. Spray and explosion characteristics of methanol and methanol-benzene blends near azeotrope formation: Effects of temperature, concentration, and benzene content. Journal of Loss Prevention in the Process Industries. 83 (2023), 105079.

[30] H. Wan, Y. Wen, Q. Zhang. Flame behaviors and explosion characteristics of two□phase propylene oxide/air mixture under different ambient pressures. Process Safety Progress. 42(1) (2023). 126-140.

[31] P K Vishwakarma, K B Mishra. Influence of sequential fireballs on thermal safety distance estimations for organic peroxide drums. Journal of Loss Prevention in the Process Industries, 75 (2022), 104683.

[32] D. O. Glushkov, K. K. Paushkina, A. O. Pleshko. Characteristics of micro-explosive dispersion of gel fuel particles ignited in a high-temperature air medium. Fuel, 313 (2022), 123024.

[33] T. M. Vu, W. S. Song, J. Park, et al. Measurements of propagation speeds and flame instabilities in biomass derived gas–air premixed flame. International Journal of Hydrogen Energy, 36 (18) (2011), 12058-12067.

[34] X. L. Gu, Q. Q. Li, Z. H. Z, et al. Measurement of laminar flame speeds and flame stability analysis of tert-butanol–air mixtures at elevated pressures. Energy Conversion and Management, 52 (10) (2011), 3137-3146.

[35] A. A. Konnov, L. V. Duakov. Measurement of propagation speeds in adiabatic cellular premixed flames of CH_4+O_2+CO_2. Experimental Thermal and Fluid Science. 29 (8) (2005), 901-907.

[36] Z. H. Wang, Y. F. Cheng, T. Mogi. Flame structures and particle-combustion mechanisms in nano and micron titanium dust explosions. Journal of Loss Prevention in the Process Industries, 80 (2022), 104876.

[37] E. Shi, J. Yu, C. Qi. Explosion characteristics and reaction mechanism of nano-aluminum/methanol fuel spray in a square closed vessel. Fuel, 357 (2024), 129928.

[38] W Wang, Y. F. Cheng, R Wang. Flame behaviors and overpressure characteristics of the unconfined acetylene-air deflagration. Energy, 246 (2022), 123380.

[39] Q. W. Zhang, Y. F. Cheng, B. B. Zhang. Deflagration characteristics of freely propagating flames in magnesium hydride dust clouds. Defence Technology, 31 (2023), 471-483.

[40] R. Wang, Y. F. Cheng, S. Z. LI Inhibitory effects of typical inert gases on the flame propagation and

structures in TiH2 dust clouds. Powder Technology, 427 (2023), 118795.

[41] F. F. Hu, Y. F. Cheng, B. B. Zhang. Flame propagation and temperature distribution characteristics of magnesium dust clouds in an open space. Powder Technology, 404 (2022), 117513.

[42] J. K. Tavares, V. Gururajan, J. Jayachandran. Effects of radiation heat loss on planar and spherical hydrofluorocarbon/air flames. Combustion and Flame. 258 (2023), 113067.

Submitted: 19.10.2024

Revised: 28.11.2024

Accepted: 09.12.2024